Ocean Systems Engineering, *Vol. 3, No. 4 (2013) 309-325*
DOI: http://dx.doi.org/10.12989/ose.2013.3.4.309

A study of internal wave influence on OTEC systems

Shan Shi*[1], Nishu V Kurup[1], John Halkyard[2] and Lei Jiang[3]

[1]*Houston Offshore Engineering, Houston, Texas 77079, USA*
[2]*John Halkyard and Associates, Houston, Texas 77079, USA*
[3]*Department of Civil Engineering, Texas A&M Univ., College Station, Texas 77843, USA*

(Received September 3, 2013, Revised November 15, 2013, Accepted November 30, 2013)

Abstract. Ocean Thermal Energy Conversion (OTEC) systems utilize the temperature difference between the surface water and deep ocean water to generate electrical energy. In addition to ocean surface waves, wind and current, in certain locations like the Andaman Sea, Sulu Sea and the South China Sea the presence of strong internal waves may become a concern in floating OTEC system design. The current paper focuses on studying the dependence of the CWP hydrodynamic drag on relative velocity of the flow around the pipe, the effect of drag amplification due to vortex induced vibrations and the influence of internal waves on the floating semi and the cold water pipe integrated OTEC system. Two CWP sizes are modeled; the 4m diameter pipe represents a small scale prototype and the 10m diameter pipe represents a full commercial size CWP. are considered in the study.

Keywords: Internal wave; OTEC System; Cold Water Pipe(CWP)

1. Introduction

Design of floating ocean thermal energy conversion (OTEC) platforms require a comprehensive analysis of the host platform motions in addition to the stress and strain of the attached cold water pipe (CWP). The offshore structural response of such systems along with the commercial feasibility of such projects has been extensively studied and is available in literature (Shi *et al.* 2012, Claude 1930, Chou *et al.*1978, Paulling 1979, Barr and Johnson 1979, Vega *et al.* 1988, Vega 1992).

The analysis of the OTEC system is usually performed by a coupled analysis approach due to the feedback of the CWP response on the platform. The approach involves analysis of the OTEC platform, mooring lines and the CWP as an integrated structure. Design environmental conditions such as waves, wind and current are then applied and the platform global motions as well as the CWP response are then obtained. However it is observed that even small discrepancies in the modeling could cause significant errors in the response of the system and could result in a faulty design.

The current paper focuses on the influence of the enhanced drag due to the vortex induced vibrations (VIV) of the CWP. The vortex induced vibration occurs due to vortex shedding arising from the current and internal wave applied to the CWP. The study focuses on both a 10 MW small

*Corresponding author, Manager Of Riser Systems, E-mail: sshi@houston-offshore.com

 ISSN: 2093-6702 (Print), 2093-677X (Online)

prototype platform with a 4m pipe as well as a 100 MW full size platform with a 10 m diameter pipe.

The study provides a benchmark on the effects of VIV induced drag on the OTEC system and assesses if the phenomenon of internal waves, which commonly occurs in several parts of the globe where OTEC systems are proposed to be installed, has any impact on the design of such systems.

2. Description of OTEC system

2.1 100 MW OTEC System

The OTEC platform used in this study is the 100 MW OTEC system shown by Lockheed Martin Corporation at the 2011 Pacific Coast Electrical Association (PCEA) Hawaii Biennial Conference (Varley *et al*. 2011). A four column semisubmersible with eight (8) power generation modules attached to the four (4) sides the semi hull is used as the platform. The profile and plan view of the system are presented in Fig. 1 below.

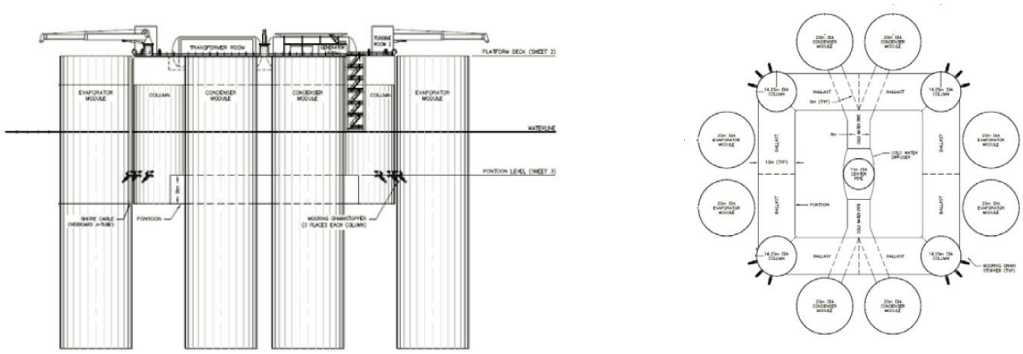

Fig. 1 100 MW OTEC platform elevation view (L) and plan view (R)

The OTEC platform is assumed to be moored in 1100 m water depth. A twelve line taut CPC (chain-polyester-chain) mooring system is used for station keeping. The polyester line has a diameter of 240 mm and is 2400 m long with a unit wet weight of 10 kg/m. The mooring chain has a diameter of 145 mm with unit wet weight of 380 kg/m.

The key parameters of the platform are summarized in Table (1) below:

The 1000 m long cold water pipe is suspended from the center/keel of the platform. The outer and inner diameter of the CWP is 10.5 m and 10 m respectively. The pipe is a one piece continuous structure and is made of composite material. It is fabricated on site of the platform and is attached to the platform via a gripper system. However it is assumed for the purposes of analysis that the CWP is rigidly connected to the platform via equivalent rotational springs of high spring stiffness.

Table 1 Particulars for 100 MW pilot plant

Particulars	Value
Topsides Weight, t	9,091
Hull Weight, t	5,864
Hull Draft, m	20
Column Spacing, m	56
Column Diameter, m	14.25
No. Of Mooring Lines;	12
Power Generation Module Draft, m	60
Power Generation Module Dia, m	20
Total Displacement, t	192,381
Displacement Semi Only, t	37,513

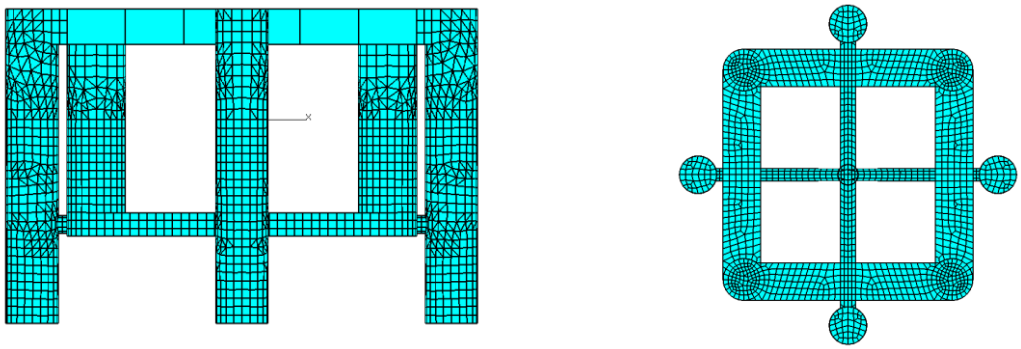

Fig. 2 10 MW OTEC platform elevation view (L) and plan view (R)

2.2 10 MW OTEC system

A 10 MW OTEC system representing a small scale prototype is also analyzed in this study for comparison purposes. It is a smaller version of the 100 MW plant with 4 remoras instead of 8.

The topside weight and hull weight are about 900 tonnes and 3600 tonnes respectively. The hull draft is 20 m with a column spacing of 50 m and a column diameter of 10 m. The remora draft is reduced to 38 m. In addition the hull is moored in place by 8 mooring lines instead of 12. The profile and plan view of the OTEC system are shown on the left and right side respectively in Fig. 2 above.

The cold water pipe is made of composite material with a total length of 1000m. It is attached to the 10 MW OTEC platform with an outer diameter of 4.2 m and an inner diameter of 4.0 m

3. Internal waves

The physics of the internal wave is essentially a counterbalance between the nonlinearity of the phenomenon and dispersive effects arising due to the differences in velocities of the different Fourier components (Ablowitz 1981).

Internal waves are found to have three different phases: generation, propagation and dissipation. The phase primarily considered in this paper is the propagation phase which is characterized by the addition of further oscillations at the rate of one per buoyancy cycle. The waves could be observed as solitons with a single oscillation or solitary trains with more than a dozen oscillations. These waves are also characterized by decreasing amplitude, phase speed and wavelength from the front of the train to the trailing edge.

3.1 Analytical model

A complete comprehensive description of the phenomenon will involve solving the full Navier stokes equation over the temporal and spatial space. Since this approach is time consuming and computationally intensive, analytical models are often used for the study of the phenomenon. The critical term in the Navier Stokes equation responsible for the internal wave phenomenon is the buoyancy term proportional to the vertical rate of change of density. If we assume that small density variations can be neglected in all terms except in terms multiplied by density (Boussinesq approximation), the equations could be further simplified.

Since this paper studies the generic effects of internal waves on OTEC systems a few approximations are adopted in formulating the theoretical model. The ocean is assumed to consist of two layers and the wavelength of the internal wave is assumed to be long when compared to the upper water depth. In addition the two dimensional quadratic Korteweg-de Vries equation for weakly nonlinear waves is adopted in the study.

Several studies where the assumptions stated above are relaxed are available in literature(Ono 1975, Joseph 1977, Liu *et al*. 1985) and while the effects of these theories on the OTEC system will be interesting, this is deferred to later work for reasons of brevity.

Korteweg-de Vries Equation and dnoidal solution In the following section the origin is taken at the at the sea surface, x is the horizontal distance from the wave source while *z* is the vertical distance from the mean water level. The equations are derived in 2D Cartesian coordinates but can be extended to 3D by a simple rotation of coordinate system.

With suitable simplifications and approximations and rescaling the Boussinesq approximation the two dimensional quadratic Korteweg-de Vries equation in Eq. (1) is obtained. (Korteweg and Vries 1895, Ablowitz and Segur 1981).

$$\frac{\partial \eta}{\partial t} + c_0 \frac{\partial \eta}{\partial x} + c_0 \gamma \frac{\partial^3 \eta}{\partial x^3} + \alpha \eta c_0 \frac{\partial \eta}{\partial x} = 0 \tag{1}$$

where η is the amplitude of the internal wave, c_0 is the long wavelength phase speed and α and γ are environmental parameters describing the nonlinearity and dispersion respectively. Although the KdV equation is characterized by the existence of multiple solutions a model termed the dnoidal model, first obtained in the context of plasma physics (Gurewitch and Pitaevskii 1973a) is adopted in this paper.

This model was utilized by Apel (2003) to investigate the propagation of internal waves in the ocean and adopted previously to study the impact of internal waves on offshore drilling units (Kurup *et al*. 2011). The notations in Apel (2003) and Gurewitch and Pitaevskii (1973b) are kept for consistency.

The mode 1 dnoidal model utilized in the internal wave formulation is presented below

$$\eta(x,z,t) = \eta_0 W(z) I(x,t) \left\{ 2dn_s^2 \left[\frac{1}{2} k_0 (x - Vt) \right] - 1 + s^2 \right\} \tag{2}$$

where s is the elliptic modulus (varies from 0 to 1), $I(x, t)$ is the recovery function capturing the recovery of the trailing edge to the equilibrium pycnocline, k_0 is the short wave length number and V is the nonlinear speed in the front of the packet. The vertical structure function $W(z)$ is modeled by the well known Taylor Goldstein equation.

$$\frac{d^2W(z)}{dz^2} + \left(\frac{N^2}{(U-c)^2} - \frac{U_{zz}}{(U-c)} - k^2\right)W(z) \tag{3}$$

where N is the buoyancy frequency, k is the wave number, U is the background current velocity and c is the phase speed. The solution to this equation in terms of normalized eigen functions $W(z)$ are obtained numerically using a matrix method by applying rigid boundary conditions to the top and bottom. The velocities and accelerations are obtained by utilizing the continuity equation and the nonlinear kinematic boundary condition. We refer the reader to Gurevich and Pitaevskii (1973a) for a detailed derivation of the dnoidal solution by asymptotic methods and Apel (1993) for the formulation in terms of the KdV environmental parameters for ocean waves.

4. Hydrodynamic drag

The inline force on a cylindrical body of unit length in oscillating flow is given by Morisons equation below.

$$F = \frac{\pi}{4}\rho C_m D^2 \dot{u} + \frac{1}{2} C_d \rho D u|u| \tag{4}$$

Where ρ is the density, D is the diameter, u is the relative velocity and C_d and C_m are the drag and inertial coefficients respectively. The first term is the inertial term while the second term computes the drag force. The drag coefficient C_d is used to quantify the drag or resistance to the body in fluid. It is found to depend on many parameters such as Reynolds number, Keulegen Carpenter number and surface roughness (White 1991).

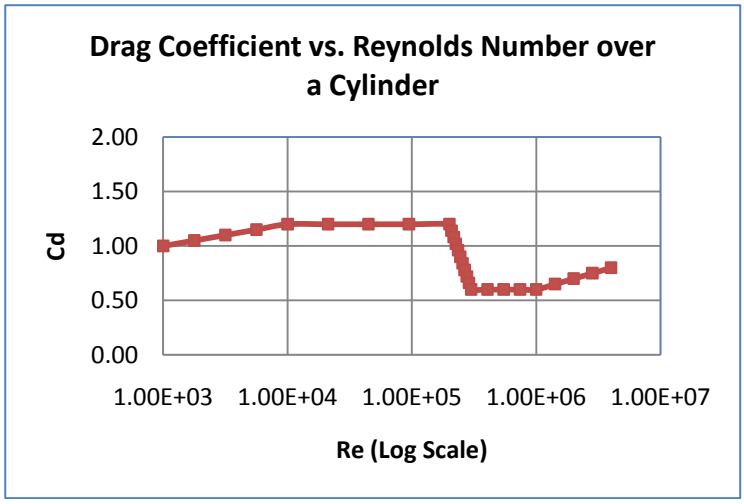

Fig. 3 Drag coefficient dependence on Reynolds number

The current paper focuses on the drag coefficient dependence on Reynolds number. Fig. 3 above shows the dependence of drag coefficient on the Reynolds number. It is seen that the drag coefficient drops in a certain range of Reynolds number called the critical flow regime. If the Reynolds number is below the critical flow regime it is called the subcritical flow regime and is characterized by the formation of laminar boundary layer. When the Reynolds number is above the critical regime (supercritical or transcritical flow) the boundary layer is turbulent beyond the separation point.

5. Vortex induced vibrations

It is seen that elastic structures like the CWP develop flow induced oscillations due to energy transfer from the flow around the body near the linear resonance area (Xu *et al*. 2013). This oscillation causes further nonlinearity by modifying the flow pattern around the body. These fluid structure interactions can lead to phenomenon like vortex induced vibrations (VIV), flutter, galloping and buffeting. The current work focuses on the vortex induced vibrations induced by the flow around the cold water pipe. There is a rich and varying source of literature on the effects of VIV on elastic structures and for a comprehensive review the reader is referred to Williamson and Govardhan (2004), Sarpkaya (2004) and references therein.

The general requirement for VIV to occur in a structure is that the vortex shedding frequency is close to the structural eigen frequency. VIV is normally a self-limiting response as opposed to galloping where large amplitude oscillations might be seen. Vortex induced vibrations are critical to design of offshore structure due to the high fatigue damage caused by the induced stresses. Vortex induced vibration are also found to increases the drag force by amplifying the drag coefficient in Morisons equation. The following empirical equation (Vandiver 1983) can be used to model the drag coefficient amplification

$$C_{D,Amp} = 1.0 + 1.043\left(2\frac{y_{rms}}{D}\right)^{0.65} \tag{5}$$

Where y_{rms} is the rms value of structural displacement and D is the diameter.

Computational analysis of VIV involves either solving the full Navier Stokes equations and the corresponding structural response within a CFD framework or using empirical models for evaluating the hydrodynamic forces which is coupled with a structural solver to evaluate the response. While the first method is more comprehensive it is computationally quite expensive and thus the second method is usually favoured for engineering design applications. There are various empirical model based programs available to perform VIV analysis of structures. The current work uses the frequency domain modal superposition program SHEAR7 to study the influence of VIV on the cold water pipe.

SHEAR7 was developed at MIT for predicting the VIV responses of beams in non-uniform flow. The program has been calibrated against data from sub critical flows and has found to be conservative in comparison test with other programs (Vandiver and Li 2005). SHEAR7 was integrated with the coupled analysis program HARP for performing the analysis on OTEC platforms.

SHEAR7 uses modal superposition to evaluate the VIV response for uniform or sheared flows (Vandiver *et al*. 2005). It performs this by balancing the input power due to lift force and the output power due to damping. The natural frequencies and mode shapes of the CWP are input

from a modal program like Flexcom7 modal module. The potentially excited modes are then determined by comparing the natural frequencies with the maximum and minimum excitation frequencies obtained via the Strouhal relationship. The excitation frequency range is dependent on user defined data for the reduced velocity bandwidth. The modes above a user defined cut-off (principally excited modes) are then found based on which the excitation length of the cold water pipe is determined. The excitation length is the length of the cold water pipe which is excited due to the power input from the surrounding fluid to the structure. If several modes are found to participate in the excitation and there are overlaps within the excitation regions, mode overlap elimination is performed. The initial lift and drag coefficients are then computed. The modal input power due to the lift force and the modal output power due to damping are then determined. The A/D (Amplitude /Diameter) ratio is computed based on the modal force and modal damping. Conservation of energy requires the input power to be equal to the output power. An iterative calculation is performed where the lift coefficient and damping coefficients are updated until the A/D ratio converges. The RMS response of the pipe is then determined from which the drag coefficient amplification can be ascertained from Eq. (5).

SHEAR7 version 4.4 is used for the computation. The user defined single and multi- mode reduced velocity bandwidth is 0.4 and 0.2 respectively. The cut-off level that determines the number of modal power in regions was set to 0.7 which is considered to be conservative.

6. Environmental parameters

Design operative conditions and internal waves observed in South China Sea are the basis of the environment conditions used in this study. A generic South China Sea field with an assumed water depth of 1100 m is selected for this study. The pycnocline is assumed to be at 200 m below the ocean surface.

6.1 Surface wind, wave and current

The maximum operative design environmental conditions listed in Table 2 below are applied in the analysis. These correspond to a 1 year return period criteria.

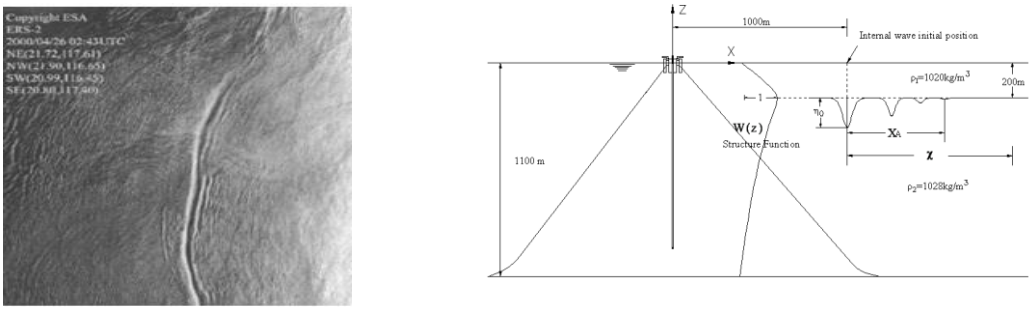

Fig. 4 Satellite picture (L) and schematic analysis model (R) of internal waves in the South China Sea (© ESA, April 26, 2000)

Table 2 Metocean data for analysis

Items	Units	South China Sea Water Depth = 1100 m 1 Year Return Period Criteria Operating Condition	
Wave		Jonswap	
Gamma		1	
Wave Direction	deg	180	
Significant Wave Height (H_s)	m	6	
Spectral Peak Period (T_p)	s	11.2	
Wind		API	
1 hour Average Wind	m/s	21.97	
Wind Direction	deg	180	
Current Profile		Normal	
		Depth	Vel
		m	m/s
		0	1.02
		-10	0.83
		-20	0.35
		-50	0.31
		-100	0.27
		-150	0.26
		-200	0.17
		-300	0.14
		-500	0.13
		-700	0.13
		-1100	0.13
Current Direction	deg	150	

6.2 Internal wave

Large amplitude internal waves generating from the Luzon Strait have been observed in the South China Sea (Fig. 4). An internal wave with wave height of 90 m (considered to an intermediate size wave in the South China Sea) was generated for the OTEC cold water pipe analysis. It is assumed that the internal wave may occur during the maximum operating wave condition for the OTEC design and analysis consideration.

The duration between the 1st peak and 2nd peak is 16.7 minutes for the 90 m wave while the duration between the 2nd peak and 3rd peak is 11.8 minutes. An internal wave developing time (T_0= 30000 seconds) is applied before the start of the coupled analysis. This time is selected to form a desired geometry of the internal wave based on observable data for coupled analysis. The internal group speed and the maximum velocity obtained at the sea water surface are 3.58 m/s and 1.31 m/s respectively.

The time history of the internal wave height, scaled velocities, and scaled acceleration distributions are presented in Figs. 5-7. The horizontal velocity is directly proportional to the vertical rate of change of the structure function [16] which causes a shearing effect near the pycnocline.

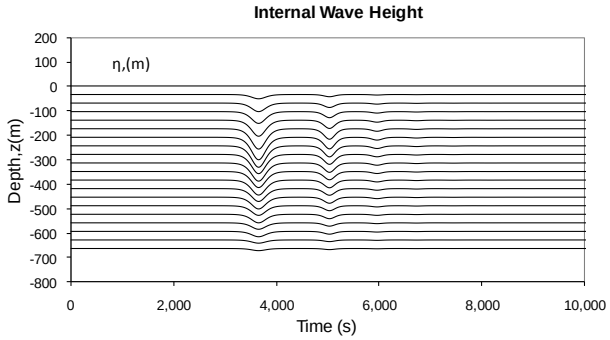

Fig. 5 Internal wave height distribution with depth (η=90 m)

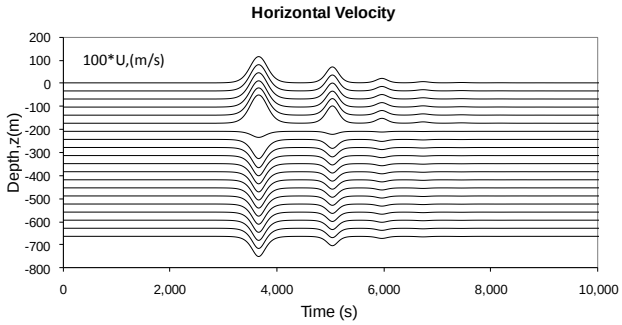

Fig. 6 Horizontal velocity distribution with depth (η=90 m)

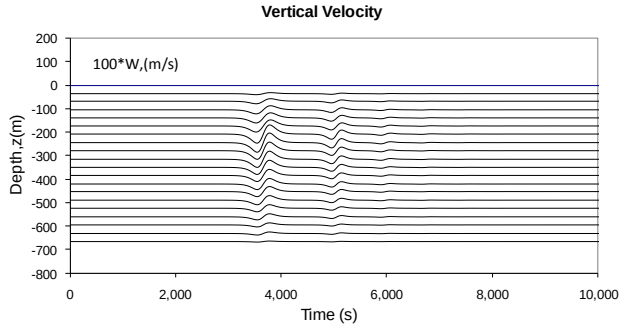

Fig. 7 Vertical velocity distribution with depth (η=90 m)

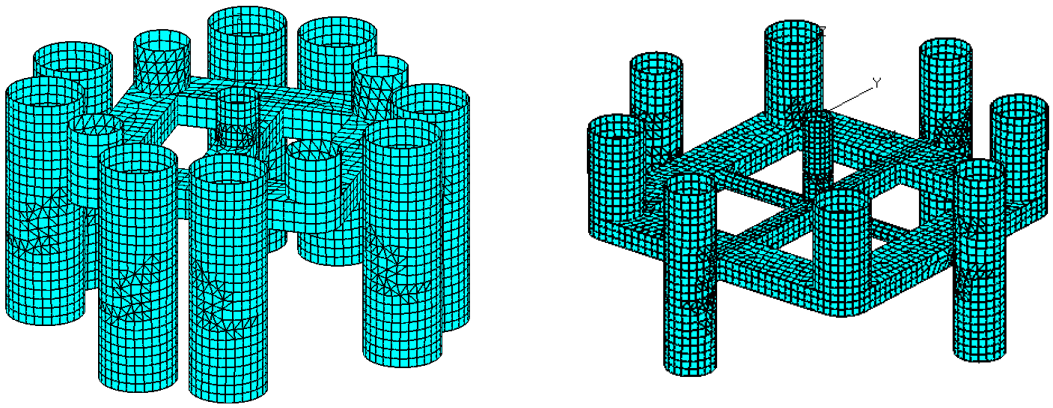

Fig. 8 100 MW (L) and 10 MW (R) OTEC hydrodynamic analysis panel models

7. Coupled analysis and modeling

The global performance analysis of the OTEC floating platform was performed with the coupled analysis program HARP to take into account the contribution of CWP to hull motions.

HARP is an integrated time and frequency domain program for coupled hull/mooring/riser system analysis (e.g., Yang and Kim 2011, Kang and Kim 2012) and was originally developed by an offshore industry JIP (Joint Industry Program). The program applies the sea wave radiation/diffraction forces calculated by program WAMIT while the contribution of internal waves is via the Morison equation. The hydrodynamic panel model used by the wave diffraction and radiation program WAMIT for both the 100 MW and 10 MW OTEC platforms are presented in Figure 8 above.

3D nonlinear beam elements are used to model the mooring lines and the CWP pipe. The platform hull is an integral part of the finite element system of solutions. The program performs dynamic finite element analysis to evaluate the offshore floating platform motions and the response of the cold water pipe. For the purposes of this study, the program was modified by integrating SHEAR7 into the code to account for the contribution of the enhanced drag amplification from the VIV in global analysis.

8. Analysis and results

Three- hour time domain simulations are performed for both the 100 MW and 10 MW OTEC platforms. Table 3 below enumerates the cases analyzed.

Table 3 Load case matrix

Otec Platform	Case #	Internal Wave	CWP Cd	VIV Enhanced Drag
100 MW	1	N/A	Cd=1	N/A
	2	Wave height=90 m, Direction =180 degrees	Cd=1	N/A
	3	Wave height=90 m, Direction =180 degrees	Cd=f(Re)	N/A
	4	Wave height=90 m, Direction =180 degrees	Cd=f(Re)	Applied
	5	N/A	Cd=f(Re)	N/A
	6	Wave height=90 m, Direction =0 degrees	Cd=f(Re)	Applied
	7	N/A	Cd=f(Re)	Applied
10 MW	8	N/A	Cd=1	N/A
	9	Wave height=90 m, Direction =180 degrees	Cd=1	N/A
	10	Wave height=90 m, Direction =180 degrees	Cd=f(Re)	N/A
	11	Wave height=90 m, Direction =180 degrees	Cd=f(Re)	Applied
	12	N/A	Cd=f(Re)	N/A
	13	Wave height=90 m, Direction =0 degrees	Cd=f(Re)	Applied
	14	N/A	Cd=f(Re)	Applied

A total of fourteen cases are analyzed for the 100 MW full scale platform (Cases 1-7) and the 10 MW prototype (Cases 8-14). The variance of drag coefficient, influence of VIV enhanced drag and the influence of internal wave along with the direction are studied based on the results from these 12 cases.

Cases 1 and 8 represent the base cases with drag coefficient C_d = 1 applied. VIV and Internal waves are not applied in those cases. The influence of the internal wave in the current direction is investigated in Cases 2 and 9. In cases 3 and 10 the influence due to dependence of drag coefficient on Reynolds number is analyzed. Cases 4 and 11 have the VIV enhanced drag additionally applied to the cold water pipes. Cases 5 and 12 are analyzed to compare the influence of Reynolds number dependent drag with the base cases. The influence of internal wave phenomenon and direction relative to applied current are analyzed by comparing cases 7 and 6 with case 4 for the 100 MW OTEC Platform. The corresponding cases for the 10 MW platform are 14 and 13 respectively.

The results of the analysis are presented in Figs. 9-14 below. The OTEC translational vessel motion statistics for all the cases are shown in Table 4 while the influence of the internal wave and direction on platform surge motion is examined in Figs. 9 and 10. The 100 MW OTEC platform is moored with 12 mooring lines instead of 8 lines for the prototype. The inertia of the hull is also considerably higher even with scaling due to the presence of additional remoras. Thus the effect of pitching due to the internal waves is considerably lesser for the full scale model compared to the prototype even though the forces and moments on the 10 m pipe would be higher.

Figs. 11 and 12 present the CWP bending moment envelope for the 100 MW and 10 MW cases respectively for all seven cases. The plot shown in the upper section of each figure is split into 3 separate zoomed plots in the lower section to enable easier comprehension of the data. The lower left plot shows the influence of the internal wave and direction with the drag enhanced VIV applied to the CWP. The lower center plot examines the influence of Reynolds number on the drag coefficient and drag enhancement due to VIV in the absence of internal waves while the lower right plot presents the same data in the presence of internal waves. The influence of internal waves

on the Reynolds number dependent drag coefficient is presented in Fig. 13 for both the 10 MW and 100 MW OTEC platforms. Fig. 14 examines the effect of internal waves on the VIV enhanced drag coefficient for both the 10 m and 4 m diameter CWP.

Table 4 OTEC vessel motion statistics

		OTEC Vessel Motions													
		100 MW							10 MW						
		Case 1	Case 2	Case 3	Case 4	Case 5	Case 6	Case 7	Case 8	Case 9	Case 10	Case 11	Case 12	Case 13	Case 14
Surge (m)	MAX	0.04	0.04	0.04	0.04	0.04	13.06	0.04	0.02	0.02	0.02	0.02	0.02	8.32	0.02
	MIN	-16.30	-50-17	-49.02	-50.34	-16.17	-15.86	-16.37	-15.66	-42.36	-40.83	-43.01	-15.38	-15.18	-15.67
	MEAN	-9.92	-12.34	-11.92	-12.49	-9.57	-8.77	-10.11	-9.41	-11.42	-10.93	-11.47	-8.99	-8.39	-9.43
Heave (m)	MAX	1.43	1.43	1.43	1.43	1.43	1.43	1.43	1.51	1.52	1.52	1.52	1.52	1.53	1.51
	MIN	-1.21	-1.20	-1.21	-1.20	-1.20	-1.20	-1.21	-1.43	-1.44	-1.43	-1.45	-1.43	-1.43	-1.43
	MEAN	0.02	0.01	0.01	0.01	0.02	0.02	0.02	-0.01	-0.02	-0.02	-0.02	-0.01	-0.01	-0.01
Pitch (deg)	MAX	1.67	1.67	1.75	1.64	1.75	1.65	1.65	1.80	2.84	2.70	3.10	1.90	1.80	1.80
	MIN	-1.46	-1.46	-1.55	-1.42	-1.55	-1.42	-1.42	-1.62	-1.61	-1.79	-1.66	-1.79	-1.62	-1.62
	MEAN	0.08	0.11	0.07	0.12	0.05	0.09	0.10	0.21	0.30	0.21	0.31	0.14	0.19	0.22

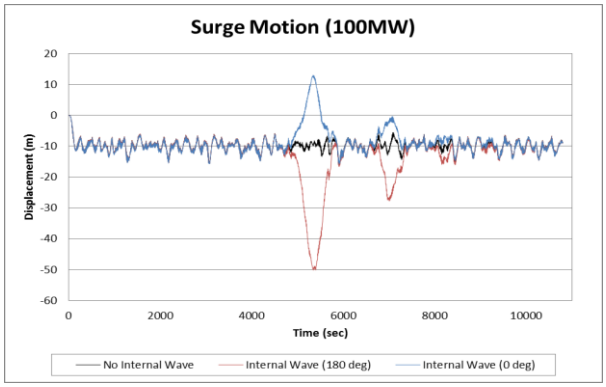

Fig. 9 Influence of internal wave and direction w.r.t current on surge motion for the 100 MW OTEC platform

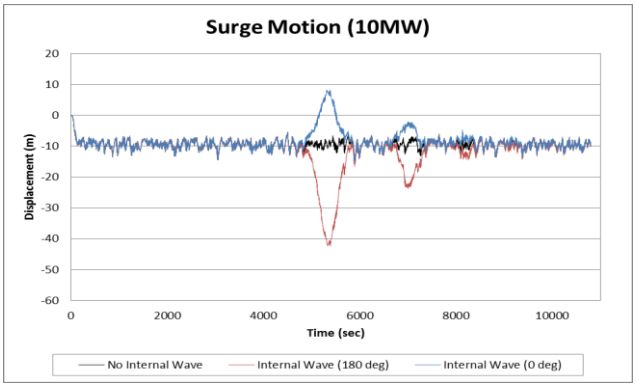

Fig. 10 Influence of internal wave and direction w.r.t current on surge motion for the 10 MW OTEC platforms

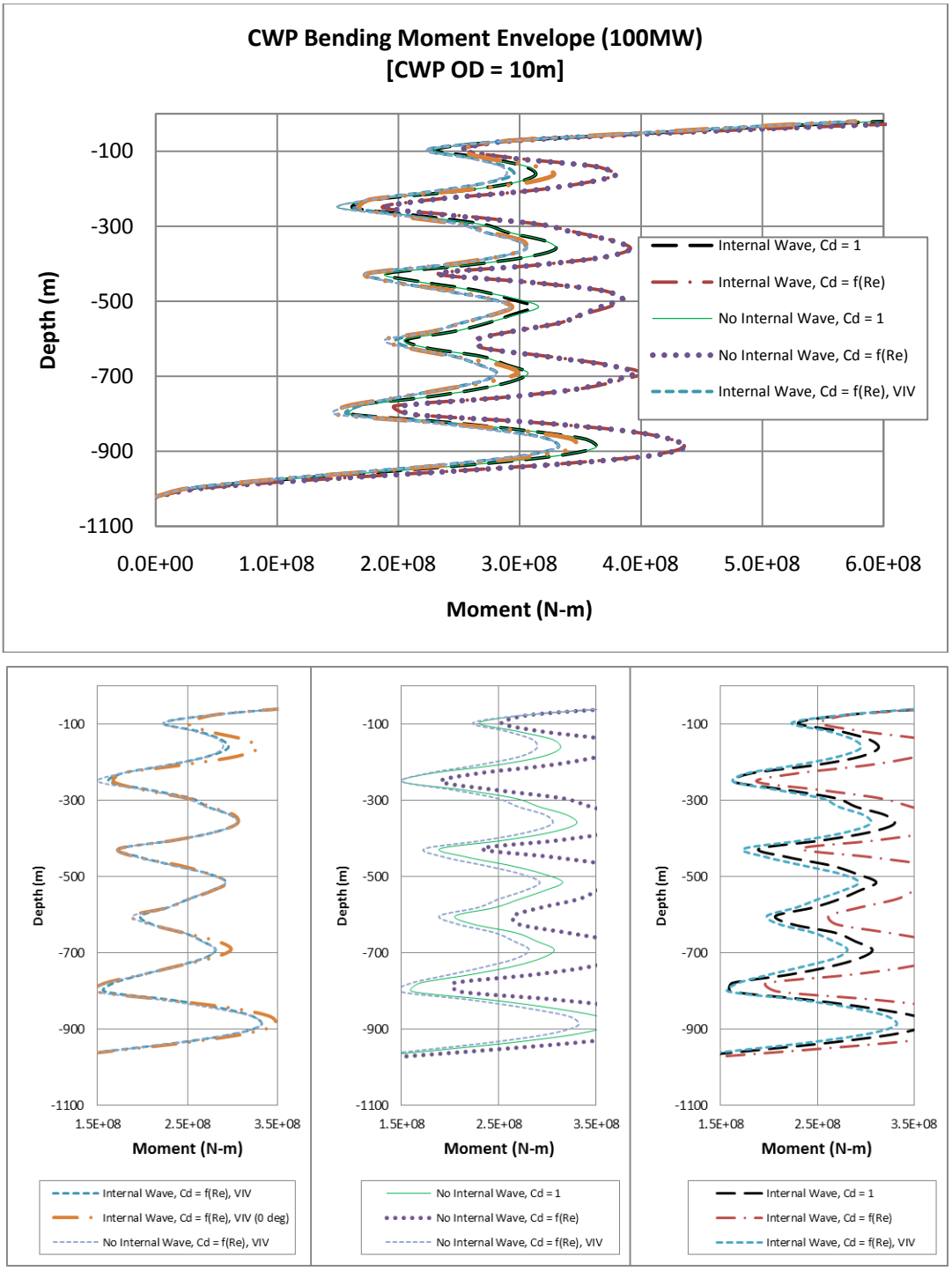

Fig. 11 CWP bending moment envelope for the 100 MW OTEC platform

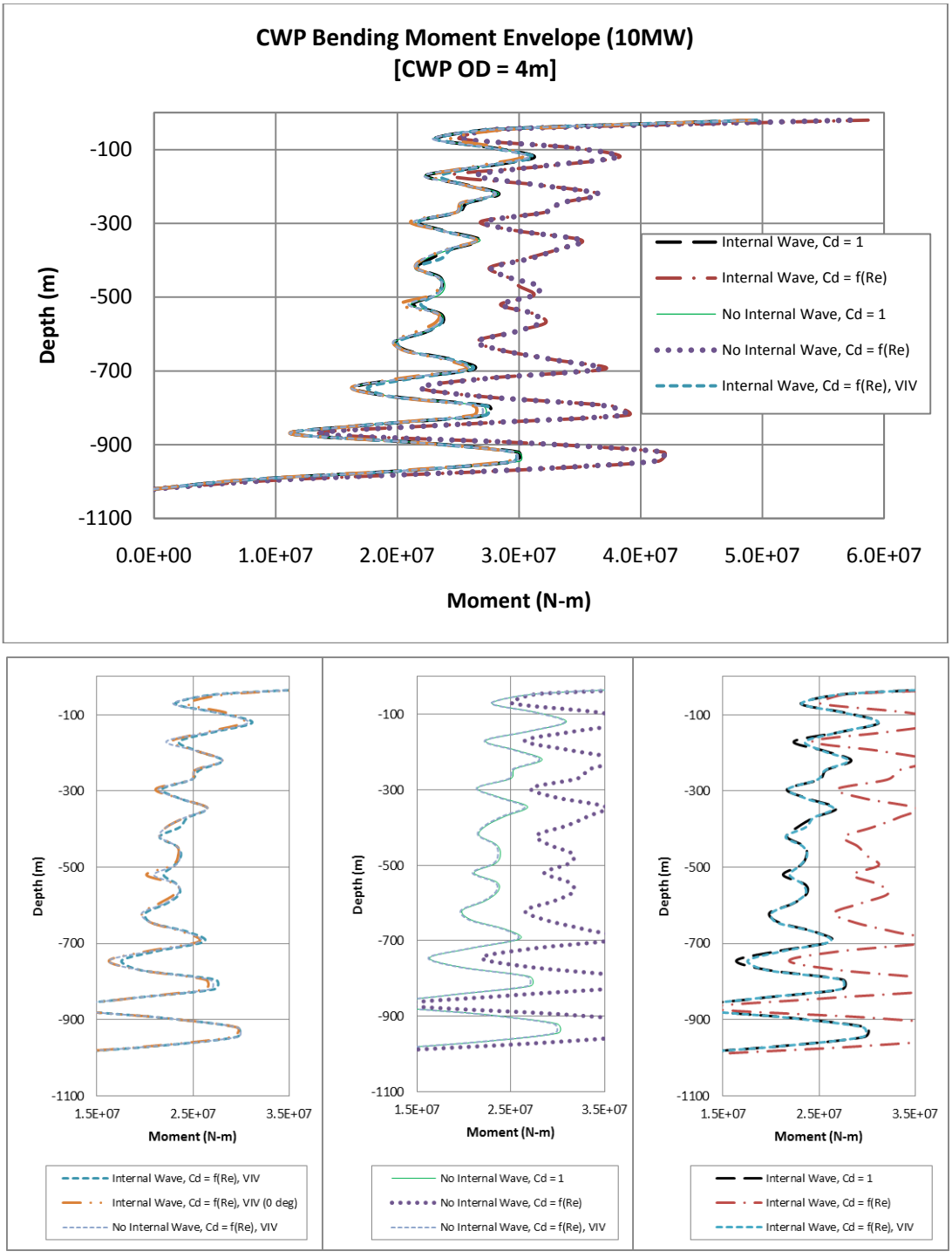

Fig. 12 CWP bending moment envelope for the 10 MW OTEC platform

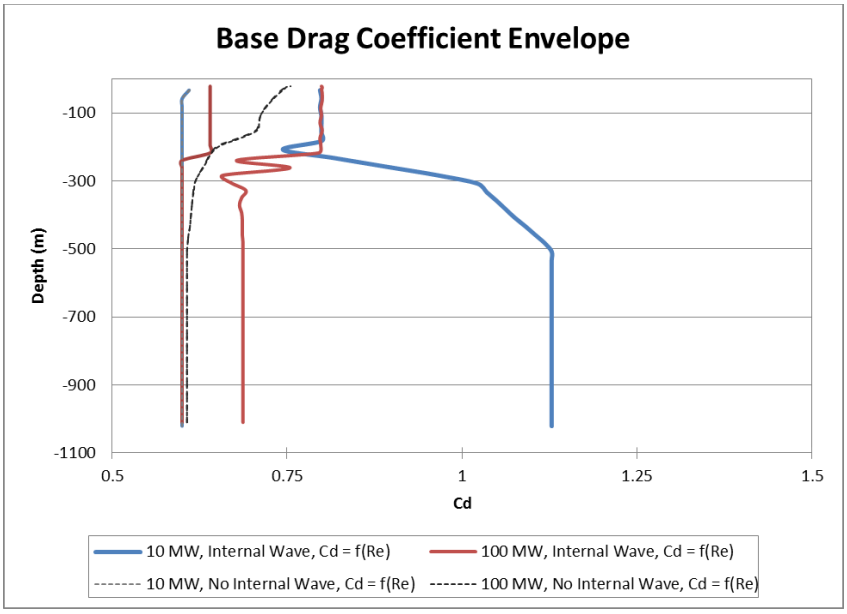

Fig. 13 Comparison of internal wave influence on base drag coefficient envelope for the 10 MW and 100 MW platforms

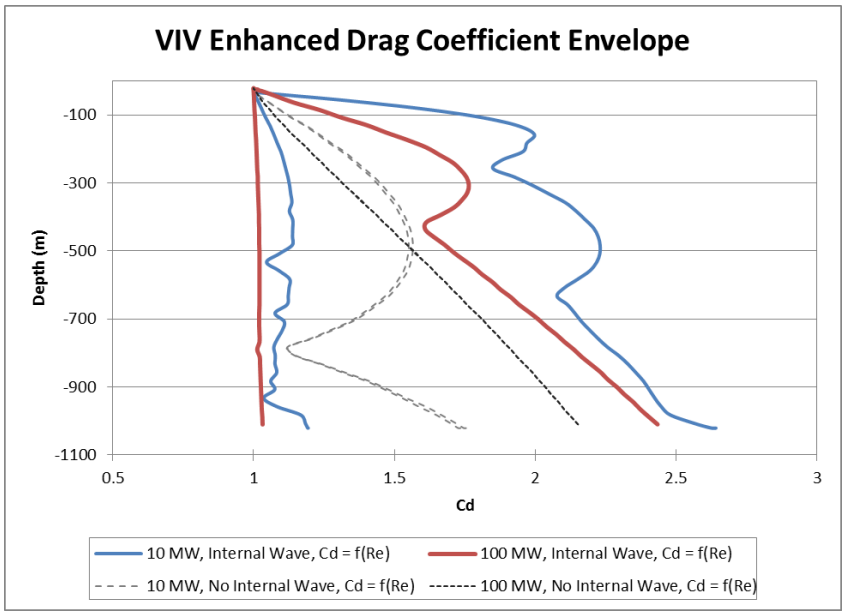

Fig. 14 Comparison of internal wave influence on VIV enhanced drag coefficient envelope for the 10 MW and 100 MW platforms

9. Conclusions

Based on the analysis results shown in the previous section, the following conclusions and findings are drawn:

(1) Modeling the CWP with the combination of the base Re number dependent drag coefficient and the VIV enhanced drag coefficient is a reasonable and effective approach to obtain the hydrodynamic drag coefficient of a larger diameter pipe in dynamic analysis.

(2) Internal wave has significant impact of OTEC platform motions and mooring line load, but there is a minimum influence on CWP dynamic bending moment for design consideration. This is because the CWP is free hanging and the internal wave period is much longer than the platform surge period due to surface wave.

(3) The larger 10 m diameter CWP will have relatively small VIV behavior than the 4 m CWP. CWP VIV under current and internal wave loads will add hydrodynamic damping and eventually could reduce the maximum CWP bending moment. But, VIV induced fatigue need to be considered for both CWP sizes.

(4) Adding strakes can be a good option for CWP to increase hydrodynamic damping and reduce VIV induced fatigue damage.

(5) For the current and internal wave applied in this study, using a combined drag coefficient of Cd equal to 1 could provide an reasonable estimation of hydrodynamic drag for the analysis.

Further validation of the results should include verification of the base drag coefficients as a function of Reynolds number for large diameter pipes. Model test data for large CWP pipes are necessary for the update. It is also useful if CFD analysis is available for the purpose of verification.

In conclusion the results obtained from this study provide valuable information for the design and analysis of future OTEC systems. The methodology of using coupled analysis with deepwater internal wave model plus the base Re number dependent drag coefficient and the VIV enhanced drag coefficient calculated by SHEAR7 program is a valid and effective approach for design and evaluation internal wave influence on OTEC systems.

Acknowledgements

The authors would like to gratefully acknowledge the support of Houston Offshore Engineering LLC for this work. The authors want to also thank Mr. Finu Lukose for his efforts on the analysis.

References

Ablowitz, M.J. and Segur, J. (1981), *Solitons and the inverse scattering transform*, SIAM, Philadelphia, PA.

Apel, J.R. (2003), "A new analytical model for internal solitons in oceans", *J. Phys. Oceanography*, **33**, 2247-2269.

Barr, R.A. and Johnson, V.E. (1979), "Evaluation of analytical and experimental methods for determining OTEC plant dynamics and CWP loads", Ocean thermal energy for the 80's; Ocean Thermal Energy Conversion Conference, 6th, Washington, D.C., June 19-22, Preprints. **1**. (A79-45776 20-44) Laurel, Md., Johns Hopkins University .

Chou, D.Y., Minner, W.F., Ragusa, L. and Ho, R.T. (1978), *Dynamic analysis of coupled otec platform cold water pipe system*, Paper #3338, *Proceedings of the Offshore Technology Conference*, Houston, May.

Claude, G. (1930), "Power from the tropical seas", *Mech. Eng.*, **52**(12), 11039-1044.
Gurevich, A.V. and Pitaevskii, L.P. (1973), "Decay of initial discontinuity in the Korteweg- De Vries equation", *JETP Lett. V*, **17**, 193-195
Gurevich, A.V. and Pitaevskii, L.P. (1973),"Nonstationary structure of a collisionless shockwave", *Sov. Phys. JETP*, **38**, 291-297.
Joseph, R.I. (1977), "Solitary waves in a finite depth fluid", *J. Phys A - Math. Gen.*, **10**(12), 225-227.
Kang, H.Y. and Kim, M.H. (2012), "Hydrodynamic interactions and coupled dynamics between a container ship and multiple mobile harbors", *Ocean Syst. Eng*., **2**(3), 217-228.
Korteweg, D.J. and Vries, G. de (1895), "On the change of form of long waves advancing in a rectangular canal, and on a new type of long stationary wave", *Philos. Mag.*, **39**(240), 422-443.
Kurup, N., Shi, S., ZhongMing, S., Miao, W. and Jiang, L. (2011), "Study of nonlinear internal waves and impact on offshore drilling units", *Proceedings of the ASME 2012 30th International Conference on Ocean, Offshore and Artic Engineering*, Rotterdam, The Netherlands.
Liu, A.K., Holbrook J.R. and Apel J.R. (1985), "Nonlinear internal wave evolution in the Sulu sea", *J. Phys. Oceanogr.*, **15**(12), 1613-1624.
Ono, H. (1975), "Algebraic solitary waves in stratified fluids", *J. Phys. Soc. Jpn.*, **39**(4), 1082-1091.
Paulling, J.R. (1979), "An equivalent linear representation of the forces exerted on the OTEC CW pipe by combined effects of waves and current", Ocean engineering for OTEC, *Proceedings of the 1980 Energy-Sources Technology Conference and Exhibition*, New Orleans, La , United States, 3-7 Feb.
Paulling, J.R. (1979), "Frequency domain analysis of OTEC CW pipe and platform dynamics", Paper #3543, *Proceedings of the Offshore Technology Conference*, Houston, May.
Sarpkaya, T. (2004), "A critical review of the intrinsic nature of vortex-induced vibrations", *J. Fluid. Struct*., **19**(4), 389-447
Shi, S., Halkyard, J., Kurup, N. and Jiang, L. (2012), "Coupled analysis approach in OTEC system design", *Proceedings of the ASME 2012 31st International Conference on Ocean, Offshore and Artic Engineering*, Rio de Janeiro, Brazil.
Vandiver , J. and Li, L. (2005a), *SHEAR7 program theory manual*, MIT, Boston, USA.
Vandiver, J., Li, L., Leverette, S. and Marcollo, H. (2005b), *User guide for SHEAR7 version 4.4 manual*, MIT, Boston, USA.
Vandiver, J.K. (1983), "Drag coefficients of long-flexible cylinders", OTC Paper 4490, *Proceedings of the Offshore Technology Conference*, Houston.
Varley, R,. Meyer, L. and Cooper, D. (2011), "Ocean Thermal Energy Conversion (OTEC)", *Proceedings of the Pacific Coast Electrical Association (PCEA) Hawaii Biennial Conference*, Presentation.
Vega, L.A. and Nihous, G.C. (1988), "At-sea test of the structural response of a large diameter pipe attached to a surface vessel", Paper #5798, *Proceedings of the Offshore Technology Conference*, Houston, May.
Vega, L.A. (1992), *Economics of Ocean Thermal Energy Conversion (OTEC)*, (Ed., R.J. Seymour), Ocean Energy Recovery: The State of the Art, American Society of Civil Engineers, New York.
White, F.M. (1991), *Viscous fluid flow*, McGraw-Hill Inc, New York.
Williamson, C.H.K. and Govardhan, R. (2004), "Vortex-induced vibrations", *Annu. Rev. Fluid Mech*., **36**, 413-455
Xu, Y., Fu, S., Chen, Y., Zhong, Q. and Fan, D. (2013), "Experimental investigation on vortex induced forces of oscillating cylinder at high Reynolds number", *Ocean Syst. Eng*., **3**(3), 167-180.
Yang, C.K. and Kim, M.H. (2011), "The structural safety assessment of a tie-down system on a tension leg platform during hurricane events", *Ocean Syst. Eng*., **1**(4), 263-283, 2011.